In situ ESEM using 3-D printed and adapted accessories to observe living plantlets and their interaction with enzyme and fungus

Romain Roulard, Michel Trentin, Valerie Lefebvre, Francoise Fournet, Ludivine Hocq, Jerome Pelloux, Eric Husson, Christophe Pineau, Loic Dupont, Arash Jamali

In situ ESEM using 3-D printed and adapted accessories to observe living plantlets and their interaction with enzyme and fungus

Romain Roulard[a,c], Michel Trentin[b], Valérie Lefebvre[c], Françoise Fournet[c], Ludivine Hocq[c,d], Jérôme Pelloux[c], Éric Husson[e], Christophe Pineau[f], Loïc Dupont[a,g] and Arash Jamali[a,*]

[a] Plateforme de Microscopie Electronique de l'Université de Picardie Jules Verne, HUB de l'Energie, rue Baudelocque, 80 039 AMIENS cedex, France

[b] FEI France, Thermo Fisher Scientific, 94454 Limeil-Brévannes, France

[c] UMRT INRAE 1158 BioEcoAgro – BIOPI Biologie des Plantes et Innovation, ,SFR Condorcet FR CNRS 3417, Université de Picardie Jules Verne, 33 rue Saint Leu, 80 039 AMIENS cedex, France

[d] PAT-Cellengo, 19 avenue de la Forêt de Haye, 54500 Vandoeuvre-lès-Nancy, France

[e] Unité de Génie Enzymatique et Cellulaire, UMR 7025 – CNRS, Université de Picardie Jules Verne, 33 rue Saint Leu, 80 039 AMIENS cedex, France

[f] Linéa Semences de Lin, 20 avenue Saget, 60210 Grandvilliers, France

[g] Laboratoire de Réactivité et de Chimie des Solides, UMR CNRS 7314, Hub de l''Energie, Université de Picardie Jules Verne, 33 rue Saint Leu, 80039, Amiens Cedex, France

* Corresponding author. Tel.: +33 3 22 82 53 23; E-mail: arash.jamali@u-picardie.fr

Abstract:

This paper describes an innovative way of using environmental scanning electron microscopy (ESEM) and the development of a suitable accessory to perform *in situ* observation of living seedlings in the ESEM. We provide details on fabrication of an accessory that proved to be essential for such experiments but inexpensive and easy to build in the laboratory, and present our *in situ* observations of the tissue and cell surfaces. Sample-specific configurations and optimized tuning of the ESEM were defined to maintain *Arabidopsis* and flax seedlings viable throughout repetitive exposure to the imaging conditions in the microscope chamber. This method permitted us to identify cells and tissues of the live plantlets and characterize their surface morphology during their early stage of growth and development. We could extend the application of this technique, to visualize the response of living cells and tissues to exogenous enzymatic treatments with polygalacturonase in *Arabidopsis*, and their interaction with hyphae of the wilt fungus *Verticillium dahliae* during artificial infection in flax plantlets. Our results provide an incentive to the use of the ESEM for *in situ* studies in plant science and a guide for researchers to optimize their electron microscopy observation in the relevant fields.

Keywords: ESEM accessories, *In Situ* observation, *Arabidopsis thaliana*, *Linum usitatissimum,* Polygalacturonase, *Verticillium dahliae*

1. Introduction:

Many macroscopic properties and qualitative characteristics of plants and biomaterials originate from their cell wall composition and organization (Holland et al., 2020). Observation of cells, tissues and organs and subtle alterations of their morphology often requires high-resolution imaging (Talbot and White, 2013). Therefore, specialized microscopy techniques have been developed to reveal structural features such as distribution of different cell types, and to characterize cell wall components at micron and submicron-scale (Mayo et al., 2010; Sozzani et al., 2014). Application of high-resolution microscopy in plant studies, however, is not always straightforward. The crucial limitations can arise from the nature of the samples and difficulties in their preparation and conservation, as well as requirements imposed by the microscopy techniques, such as specific imaging environment and complex image reconstitution (Costa and Plazanet, 2016; Wu and Becker, 2012). Scanning electron microscopy (SEM), ever since the early days of its application by biologists, has been widely used to observe plant cells, tissues and their surface morphology (Carr and Carr, 1975; Stant, 1973). SEM can provide high-resolution pseudo-three dimensional (3D) images of the surfaces at a broad magnification range. These images are acquired more rapidly and comprehended more easily than those obtained by more complex techniques used in two or three-dimensional microscopic analyses of plant cells (Barbier de Reuille et al., 2005; Costa and Plazanet, 2016). Nevertheless, the application of conventional SEM to study the surface of hydrated tissues or living cells has some limitations. Hydrated samples can lose their water in an uncontrolled dehydration process when exposed to vacuum of the microscope chamber, often resulting in deformation or destruction of their native structure (Bogner et al., 2007; Bozzola and Russell, 1999). Plant materials have usually a very high water content and are strongly dependent on turgor pressure for their structural integrity (Ensikat et al., 2010; Sorbo et al., 2008). Therefore, sample preparation is crucial in order to conserve structural features of plants tissues and cells for observation under the high vacuum of an electron microscope (Pathan et al., 2010). Accordingly, specialized sample preparation protocols have been developed to minimize the artefacts and artificial changes that may occur in the original structure of the hydrated samples during their conservation process (Ensikat et al., 2010; He et al., 2019; Kirk et al., 2009; Popielarska-Konieczna et al., 2010). These methods however, are not suitable for *in situ* observation and analyzing the live plant tissues in their native state

(Tihlaříková et al., 2019). Development of environmental SEM (ESEM), first commercialized by ElectroScan and later by Philips/FEI (Amsterdam, the Netherlands) in the 1980s, introduced the possibilities of imaging wet objects in a gaseous environment with no prior specimen preparation (Donald et al., 2003; Gilpin, 1997; Muscariello et al., 2005). In an ESEM, the hydration state of the specimen is maintained by simultaneously controlling its temperature and the water vapor pressure in the chamber (Donald, 2003; Stokes, 2008). The ESEM, therefore, has been widely used in biological research including plant science to study the ultrastructure and the morphology of hydrated samples (Stabentheiner et al., 2010), and the use of ESEM in comparative studies of static morphology of biological materials has received considerable attention. Nevertheless, the observation of dynamic processes in biology has been largely confined to the *in situ* mechanical testing of tissues or physical interactions with biological surfaces such as wetting behaviors (Dauwe et al., 2021; McGregor and Donald, 2010; Stabentheiner et al., 2010; Wigzell et al., 2016). Attempts have been made to test the viability of plant cells and view dynamic natural processes in living tissue using ESEM. Zheng et al. (2009) could maintain the cells of the upper epidermal tissue of *Allium cepa* (onion) hydrated and viable inside the ESEM chamber. McGregor and Donald (2010) successfully recorded the stomatal movements in freshly-cut leaf tips of *Tradescantia andersonia* (Spiderwort) which are regarded as robust tissues with suitable stomatal movements for ESEM imaging. Such ESEM observations were realized by controlling the physiological temperature and adjusting the water vapor pressure with the thermodynamic constraints in the chamber and minimizing the electron beam damage (McGregor and Donald, 2010). In fact, achieving a precise and careful control of chamber's conditions to maintain the sample in its natural state is complex and often counted as the main concern for performing *in situ* observation in the ESEM (Kirk et al., 2009). Furthermore, the optimal working conditions for biological applications are always sample-specific and determined empirically, which prevents the standardization of ESEM methods (Tihlaříková et al., 2019). Consequently, despite the strong interests in using ESEM for studying the plants cells and tissues, application of ESEM by the plant science community has not yet reached its full capacity. For example, the use of ESEM for monitoring the time-course of changes in plant cell walls and tissues during growth has not been reported. Limitations in maintaining the plant sample viable during examination and lack of commercial accessories dedicated to such analyses have been considered as the major hindering factors for these applications (Kwon et al., 2019; Zhang et al., 2020). In this study,

we modified a commercially available sample holder of an ESEM and optimized the chamber condition and imaging parameters for *in situ* observation of living plant cells and tissues. We describe how we obtained electron microscopic images during early growth stages of living model plants i.e. *Arabidopsis thaliana* and flax (*Linum usitatissimum*). We also show the effect of polygalacturonase (PG), a biopolymer-modifying enzyme, on cell wall structure of *Arabidopsis,* and illustrate the fungal colonization of roots of flax seedlings and invasion of the epidermal cells by the hyphae on the living plant surfaces.

2. Materials and methods

2.1. Environmental scanning electron microscopy (ESEM) and accessories

2.1.1. ESEM and Low vacuum modes

We used a Quanta 200 field emission gun environmental scanning electron microscope (ESEM, FEI Company, USA). Environmental (ESEM) and low vacuum (LoVac) modes of this SEM allow the users to image samples in a gaseous environment using Pressure Limiting Apertures (PLA) and cones. The standard configuration of the environmental mode requires installing a gaseous secondary electron detector (GSED) and a thermoelectric cooling (Peltier) stage that can operate in a temperature range from -25°C to 55°C. The desired relative humidity (RH), when using water vapor, is obtained by controlling the pressure of the ESEM chamber from 10 Pa (0.075 Torr) to 2700 Pa (20 Torr) and the temperature of the sample by the thermoelectric controller of the Peltier stage (FEI Company, 2010). These adjustments are made using liquid/gas phase border according to the relative humidity isobar. The phase diagram of pure water and the isobar chart are presented in supplemental Figure S1. In the low vacuum mode a large field detector (LFD) is used and the pressure ranges from 10 Pa (0.075 Torr) to 130 Pa (0.97 Torr).

2.1.2. Cooling stage

The Peltier cooling/heating stage in the ESEM is used to control the sample's temperature within 20 °C around the ambient, ranging from – 25 °C to + 55 °C. This stage can be used to create water condensation on the sample surface and achieve 100% relative humidity (RH) with respect to the water vapor pressure of the chamber (FEI Company, 2010). The original cooling stage provides a support for a standard cylindrical ESEM sample holder with diameter

of 10 mm (Figure 1a and 1b). This emplacement is sufficient for holding small-sized samples such as *Arabidopsis* and flax seeds, however, it does not provide enough surface to accommodate growing seedlings of these species. Upon germination of the seeds, the seedlings grow rapidly and within a few days can reach the edge of the sample holder (Figure 1c). Therefore, we aimed to assemble a new module with increased surface area that could hold a bigger ESEM mount to accommodate the growing seedlings. We first dismounted the original cooling stage and specified the dimension and technical details of its components. Based on the original design and according to the microscope manufacturer's requirements, new pieces were redesigned and fabricated. Autodesk Fusion 360 software (Autodesk, Inc., San Rafael, CA, USA) was used to design all the components and develop 3D models. The designed pieces were saved in stl. format and machined from stainless steel and aluminium or fabricated with PVA filament using a Prusa MK3 3D-printer (Prusa Research, Czech Republic). Electronic parts and wires were purchased from the local stores. Technical details of the original and new designed accessories are provided in supplementary materials (supplemental Figure S2).

2.1.3. Bio-transfer module

We designed a simple specimen holder (hereinafter referred to as "bio-transfer module") that could fit the modified cooling stage. Two prototypes of a bio-transfer module were assembled. The first prototype included a base composed of a 3-dimensional printed plastic ring and an aluminium cylinder with a diameter of 25 mm that provided ≈5 cm^2 metal contact surface with the Peltier module (supplemental Figure S3). In this model, the plastic part can be replaced by other materials for specific applications, for example, glass or alternatively shatter-resistant acrylic glass to increase the exposed surface to light as required for germination of some plants seeds (Toole et al., 1955). In the second prototype, the whole base of the bio-transfer module was machined from aluminium providing ≈10 cm^2 of metal surface. The larger metal surface in the latter model, which was then used throughout this study, provides a high electronic conductivity enabling the analyses of larger specimens and using higher accelerating voltages during observation. A transparent cover composed of polycarbonate permitted light transmission to the seedlings and their protection against contamination during their growth and transport (supplemental Figure S3).

2.2. Biological samples

2.2.1. *Arabidopsis thaliana* and Polygalacturonase enzyme

Arabidopsis thaliana (A. thaliana) is a model plant with a fully-sequenced genome and many interesting characteristics such as a short life cycle, prolific seed production, and numerous mutant lines (The *Arabidopsis* Genome Initiative, 2000). We used the ESEM to study the cells of elongated hypocotyls in etiolated seedlings and their modification after exogenous application of heterologously expressed enzymes. Pectin depolymerizing enzymes such as polygalacturonases (PG) can induce pectin remodeling and affect cell elongation and integrity (Hocq et al., 2020). Here we added an *Arabidopsis* polygalacturonase (AtPG (endo-PG, EC 3.2.1.15)) into the growth medium of *Arabidopsis* to observe the induced modifications on the cells on the hypocotyl surfaces. The active enzyme was expressed heterologously in the yeast *Pichia pastoris* X-33 strain and purified as previously described (Hocq et al., 2020). *Arabidopsis* seeds were surface sterilized, soaked in 1mL water and placed for 2 days in a cold chamber for stratification. Seeds were then placed to germinate in sterilized 24-microwell plate containing a ½MS semi-solid medium plus either active or inactivated (control) enzymz (8µg AtPG /600µL/well). Microplate containing the seeds were first exposed to 6 hours of flash light (120µmoles/m²/s), then positioned vertically in the dark for 48-72 hours to favor the straight elongation of the hypocotyls (Desnos et al., 1996). The 2-days old seedlings were carefully transferred into the sample holder for ESEM observations.

2.2.2. Flaxseeds and seedlings

Flax (*Linum usitatissimum* L.) is an important agricultural plant with an increasing application in nutraceutical and bio-pharmaceutical industries, fibers, human food and animal feed. Many interesting characteristics of flax are influenced by its seeds germination and seedlings properties (Dauwe et al., 2021; Jhala and Hall, 2010; Wang et al., 2015; Wang et al., 2016). The seeds of brown flax (cv. Baladin), kindly provided by the seed company Laboulet (Airaines, France), were visually screened and those with similar sizes and weights were selected as the experimental material. Flax seeds were germinated on wet filter paper in 90-mm-diameter Petri dishes as described previously (Dauwe et al. 2021) or directly in the bio-transfer module. After 48h growth in the dark, they were then transferred to a phytotron chamber and grown under controlled conditions (at 23°C and 80% humidity) using a light-dark cycle (16h:8h) with

209 a light intensity of 3350 lux to 3500 lux. These seedlings were then transferred into the ESEM
210 using the bio-transfer module for microscopic observation.

211 2.2.3. *Verticillium dahliae*

212 *Verticillium dahliae* is a fungus that causes *Verticillium* wilt in many crops plant. This fungus
213 predominantly infests the fiber flax cultures in northern France causing significant yield losses
214 (Blum et al., 2018). We have artificially infected the flax seedlings using an undisclosed
215 protocol developed by the company "Linéa Semences" (Grandvilliers, France). Briefly, this
216 protocol consists of inoculation of roots of two-week old flax plantlets grown under controlled
217 conditions (as above) with a spore suspension of *V. dahliae* grown on a potato dextrose agar
218 (PDA) medium for 7 days. Using ESEM, we observed the native fungal structure and
219 morphology in their hydrated culture medium, and studied the interaction of fungus mycelium
220 with plantlets by imaging the epidermal and cortical cells of artificially infested plants.

221 **3. Results and discussion**

222 3.1. Modification of accessories
223 *In situ* observation of samples such as hypocotyls of *Arabidopsis* and germinated flaxseeds and
224 their growing plantlets necessitated modification of the standard thermoelectric cooling
225 stage. The hydration of a specimen in the ESEM was controlled by the temperature and the
226 pressure of water vapor in the microscope chamber. The pressure control of the ESEM
227 chamber is achieved by the use of differential pumping system and pressure-limiting apertures
228 (PLAs), and the temperature of the sample is adjusted by a cooling stage operating by Peltier
229 effect (Stokes et al. 2008). For an accurate control and reading of the sample's temperature,
230 we aimed to maximize the contact of the samples with the holder by redesign of the cooling
231 stage. The holder is in contact with a thermoelectric (Peltier) cooling device that is typically
232 manufactured from two thin ceramic wafers which sandwich a series of p and n doped
233 bismuth telluride (Bi_2Te_3) semiconductor materials. The ceramic material on both sides of the
234 thermoelectric device adds rigidity and the necessary electrical insulation. When current
235 passes through these elements, one side of the wafer heats and the opposite one cools, and
236 reversing the polarity switches cold and hot sides (Supplemental Figure S2) (FEI Company,
237 2010; Shourideh et al., 2018). In our redesigned module, we have replaced the original Peltier
238 device (10 x10 mm^2) with a larger one (30 x30 mm^2) that could consequently receive a larger

mount recipient with the diameter of 25 mm. The mount recipient is a plate into which the sample holder is inserted. A thermistor (PT 100, RS components, UK) was placed inside of the new mount recipient to give an accurate temperature reading in close vicinity under the sample. The mount recipient was installed on the new Peltier using a thermal grease. The inner cable and water hoses were then connected to the base of the stage to pass the current and remove excess heat efficiently as required by the microscope manufacturer. The details on the configuration and dimensions of the new module are presented in supplementary data (Supplemental Figure S2). The functionality of the new assembly was confirmed by comparison of temperature and water condensation and evaporation rate of this module with that of the standard module in an identical condition. Figure 2 shows the original cooling stage module and the modified design allowing comparison of the surface areas of the two modules regarding their provided surface areas (Figure 2). The higher surface contact and temperature exchange area of the new cooling stage module, enabled us to assemble a compatible specimen bio-transfer mount to transfer the germinating seeds and growing seedlings to the SEM chamber with minimal change in their natural posture. In such way, samples in the bio-transfer module could be transported into and out of the microscope with minimal dislodgement or loss of their contact with the holder. As discussed later in the following sections of this paper, such a configuration enabled us to maintain the sample in their native state during the ESEM observation and analyze the structure and organization of the cells and the effect of the enzyme and fungus on their morphological aspects during the early growth stages of the seedlings.

3.2. Observation of live plantlets

3.2.1. Optimization and imaging

We first optimized the imaging parameters and the chamber condition of the microscope to observe the native structure of very small seedlings of *Arabidopsis*. In dicotyledonous seedlings, the hypocotyl is part of the stem between the root and the cotyledons and is widely used as a model for the physiological study of the mechanism of cell elongation and variety of other biological events (Gendreau et al., 1997). The young etiolated hypocotyls with a diameter smaller than 250 µm and a length varying between 2 to 20 mm are very fragile and known to be highly susceptible to changes of relative humidity (Burgert and Keplinger, 2013).

As a reference, we therefore began by analyzing young hydrated etiolated *Arabidopsis* seedlings (2-days old dark-grown) to obtain images of their surfaces and cellular structure. Theoretically, hydration of the samples in the ESEM is achieved by setting the microscope to a specific water vapor pressure and cooling the specimen to the relevant temperature indicated by the phase diagram of water (as described above, supplemental Figure S1). In practice, however, the young plantlets were greatly impacted before reaching the desired relative humidity, because of dehydration during the pump-down and evacuation of the air from the chamber. This resulted in deformation of cells in hypocotyls and other organs such as roots and testa (Figure 3a-d). We could mitigate this issue by cooling the sample down to the target temperature and adding several drops of ultrapure water to the stage base before closing and pumping down of the chamber. Furthermore, purging water vapor into the specimen chamber (five cycles) during pump-down could improve saturating the sample's surroundings to prevent dehydration before reaching the designated chamber pressure. These steps have previously shown to be effective in preventing dehydration of desiccation-sensitive samples in the ESEM (Jenkins and Donald, 2000). We observed that the overall structure of the live seedlings was preserved in the ESEM chamber when the relative humidity was maintained around 85% (Figure 3e), conforming to their structural characteristics previously revealed in the fixed samples (Gendreau et al., 1997). At lower RHs the hypocotyl structure was extensively deformed (Figure 3f). We could achieve high levels of RH, by maintaining the temperature at 20 C° and adjusting the pressure to 14 torr. Higher vapor pressures could reduce the charging effect and proved to be essential for preserving the tissues of the fragile seedlings, however, further increase in the relative humidity compromised the sharpness of the image with significant loss of resolution. Moreover, condensation of vapor formed droplets and films of water on the surface of the specimens (Figure 3g), which obscured the underlying structure and reduced contrast as previously reported for ESEM observations (Jansson et al., 2013; Jenkins and Donald, 2000). Details on optimal image acquisition parameters of *Arabidopsis* seedlings are summarized in Table 1. Optimization of imaging parameters for ESEM analyses of the sensitive hypocotyl cells provided reference points to observe other cells and tissues of the seeds and small seedlings of *Arabidopsis*. Figure 4 shows examples of ESEM images of diverse organs and cells including germinating seed surfaces and collumella of their mucilage secreting cells and cotyledons, root and shoot apical meristems, trichomes, stomata, rhizoderm cells and extremely delicate root

hairs in the growing seedlings. Theses ESEM images of *Arabidopsis* organs and cells conform to the previously reported SEM images that were obtained from the chemically-fixed tissues (Byrne, 2006; Pillitteri and Dong, 2013; Tsukaya, 2013). Our ESEM results not only show the disposing of sample preparation steps that are required for classical SEM observations, but also the ability of this approach to accurately study the surface morphology and anatomical development of the cells in their native state in the live growing seedlings.

3.2.2. Time course *in situ* ESEM and repetitive observation of growing plantlets

To observe the early stages of seedling growth and development on a daily basis by *in situ* ESEM, we combined our home-designed cooling stage and bio-transfer module. The flax seeds germinated readily in the bio-transfer module in a phytotron. The module containing germinated seeds could be easily transferred to the ESEM chamber and fitted on the newly designed cooling stage. We could subsequently image diverse cells and tissues and follow their time-course of modification in the germinating seeds and seedlings (Figure 5), then return the module back to the phytotron after observation. Similar to our ESEM observation of *Arabidospis* seedlings, imaging of flax seedlings also required an adjustment of the acquisition parameters for different tissues and cells. The combination of the optimal parameters used for ESEM imaging of different parts of the living seedlings of *Arabidopsis* and flax are outlined in Tables 1. Natural resistance of plant tissues to dehydration and beam damage varies by their types and upon their growth (Stabentheiner et al., 2010). Structures such as seeds or pollens are usually tolerant to desiccation in most plants, however, there is a great variation in the resistance and deformation of vegetative tissues upon dehydration (Oliver, 1996; Wakui et al., 1999). We found that, the *Arabidopsis* hypocotyls were more resistant to partial vacuum in older plantlets and could be observed under low vacuum (pressure not exceeding ~1 torr) after a week of germination without showing significant structural deformation. The increase of the cell wall thickness following the expansion of the thin primary cell walls in growing plants, could play a role in the resistance of the older plant to the vacuum and dehydration (Kumar et al., 2016; Vicré et al., 2004; Vogler et al., 2015), and therefore to the partial vacuum or oscillation of the humidity in the microscope chamber during analyses (Burgert and Keplinger, 2013; Treitel, 1949). Furthermore, cuticle that is a complex structure mainly composed of a lipid polymer, i.e., cutin and waxes, coats the outermost layer of periclinal cell walls of all aerial organ epidermal cells. The cuticle layer provides a barrier to prevent non-

stomatal water-loss, and plays various roles in response to environmental stresses (Jacq et al., 2017; Yeats and Rose, 2013). This could also explain why it is possible to observe older plant tissues and cells by SEM at lower pressure i.e. low vacuum mode. We observed that the roots, even in older seedlings, suffered more easily from dehydration caused by the partial vacuum in the microscope. We could prevent this dehydration by wrapping the roots with blotting paper soaked in water. The lack of a strong diffusion barrier, such as cuticle, at the surfaces of epidermis cells in the primary growth stage could explain the higher sensitivity of the roots to the variation of humidity of the ESEM chamber compared to aerial plant organs (Berhin et al., 2019). Beside appropriate operation parameters to maintain the tissue fully hydrated, the viability of cells depend on the beam intensity, particularly in relation to the beam accelerating voltage and the total electron dose (Zheng et al., 2009). During the imaging process, the image acquisition parameters such as working distance, acceleration voltage, scan speed and spot size were optimized to minimize beam damage to the living cells (Table T1). The images were generally recorded at acceleration voltages between 5 and 20 kv and a working distance between 5 to 10 mm. The beam was blanked during imaging intervals to reduce the beam damage to the samples and visible artifacts that could occur during ESEM observation as previously reported (Dobberstein et al., 2005). Our post-ESEM surveying of the seedlings that underwent such repetitive exposure to the vacuum and electron beam showed that they maintained their vitality and vigor and continued their growth and development (Supplemental Figure S4). Nevertheless, the growth rate of these plantlets was found to be slightly lower compared to those that had not been observed in the ESEM. Furthermore, during our repetitive observations, we occasionally noticed the occurrence of epidermal meristems on the hypocotyls (Figure 5, D9 b). The presence of such meristems has been previously attributed to the exposure of seedlings to drought or radiation stresses (Tafforeau et al., 2004). These findings could indicate the presence of stresses in the underlying cells that remain undetectable at the surface. Such damage can occur, for example by an increase in the reactive oxygen species (ROS) or the rupture of plasma membranes (Bandurska et al., 2012; Muscariello et al., 2005; Zheng et al., 2009), which may be triggered in the ESEM chamber due to the formation of free radicals through electron beam interactions or pressure oscillation. Faster image acquisition could prevent possible beam and thermal damage to the samples, however, it compromised the signal to noise ratio and lowered the quality of the images. It should be noted that the insertion of pressure limiting aperture (PLA, 500 µm) on the pole

piece, essential for ESEM operation, limited the field of view and restricted the lowest magnification to around 200x. Increasing the working distance and subsequently acceleration voltage to compensate the beam scattering and the weak signals, could provide a larger view, albeit at the expense of optimization time for imaging in the wet conditions of the chamber (Muscariello et al., 2005).

3.2.3. Effect of enzyme application on hypocotyl structure

ESEM permitted us to observe the overall structure of hypocotyls and, in greater detail, identify the individual cells and their boundaries in the live seedlings without any sample preparation (Figure 4). The etiolated (dark-grown) seedlings of living *Arabidopsis* (wild type Col-0) featured typical morphological phenotypes such as apical hook, hypocotyls, unexpanded cotyledons and short root (figure 4d-f) in accord with the results of previous SEM studies on cryogenically-prepared samples (Desnos et al., 1996; Gendreau et al., 1997). The hypocotyls' cells in etiolated seedlings of *Arabidopsis* are known to have a simple anatomy and a postembryonic growth that is exclusively the result of a controlled series of cell-elongation events (Desnos et al., 1996; Gendreau et al., 1997). Such characteristics could make this organ an apt model to study the effects of diverse growth factors on cell elongation. We used heterologously expressed AtPG, a PG (EC 3.2.1.15) that induces pectin remodeling (Hocq et al. 2020) to illustrate structural modification of hypocotyls cells. Our ESEM analyses revealed that the presence of active AtPG, modified the integrity of the hypocotyls by impairing the longitudinal and ultimately transversal adhesion of cell walls in treated seedlings (Figure 6b and c), more apparently in epidermis cells and occasionally in their underlying cortex cells (Figure 6 c). The hypocotyls of the control seedling grown with inactivated AtPG (denaturated protein) did not show any separation of the adjacent cells (Figure 6 c). These ESEM observations are comparable to the observation we made on cryo-prepared samples using low-vacuum SEM and light microscopy as shown in Figure 6 (d-i) and accord with the results of prior studies on the relation between the role of polygalacturonases in modification of cell wall rigidity and elongation (Sénéchal et al., 2014). Polygalacturonase is a pectin lytic enzyme implicated in cell expansion and elongation by degrading pectin in plants cell walls. This enzyme hydrolyses the α-1,4-linked-D-galacturonic acid units which compose the homogalacturonans (HG), the major polymer of pectins (Babu et al., 2013; Hadfield and Bennett, 1998; Xiao et al., 2014). Our finding on separation of the cells could be attributed to

the softening and decomposition of pectin in HG-rich middle lamella of the cells by PGs, however, the exact function of these enzymes during cell elongation is not known (Zhang et al., 2021). During our observation, we noted that the AtPG-treated hypocotyls were more sensitive to the vacuum of the ESEM compared to the untreated ones, probably because of the enzyme's effect on the loss of integrity of the epidermal tissue and weakening of their mechanical properties. The vulnerability of such organs in the ESEM environment, could be mitigated by increasing purge cycles during the pump-down of the chamber and faster image acquisition during observations as described above. Our method of observation shows promise as a means of analyzing and illustrating the structural modification of living cell walls of plantlets upon the application of biopolymer-modifying enzymes and this may lead to broader use of this technique with the increasing interest in the *in situ* enzymatic treatment of plant cells.

3.2.4. *In situ* plant-fungus interaction

We could observe a laboratory culture of *Verticillium dahliae* mycelium in its native state in the ESEM. *In situ* observation of the structure of mycelium networks of this pathogen in the culture medium and then its identification during its development in infected plantlets (Figure 7a-i) was performed by optimization of imaging parameters at a relative humidity of 75% (Table 1). *V. dahliae* is a soil borne pathogen and belongs to the fungal class Deuteromycetes (Fungi Imperfecti), a group of fungi with an unknown sexual stage. We imaged the vegetative part of this fungus, by which it spreads in plants, and could identify different hyphal structures such as conidium, conidiophore and phialide in the fungal colony in the medium (Figure 7b and c). The structural and anatomical information on the fresh fungus provided by the ESEM observation in their native state accord with those previously reported on the chemically-fixed samples from isolated *V. dahliae* obtained by optical or scanning electron microscopy (Babu et al., 2013; Inderbitzin et al., 2011). ESEM therefore could avoid the time-consuming sample preparation and thus had advantages over other imaging techniques for *in situ* studies. Attention should be paid, however, to the high sensitivity of fungal cells to dehydration and their low intrinsic contrast during their ESEM analyses (Kaminskyj and Dahms, 2008). Our observation of the infected seedlings showed that the fungus surrounded the roots with a thick mantle of closely interlaced hyphae (Figure 7d-f). The hyphae expanded to the higher parts of the plantlets and colonized stem (hypocotyl) and leaves (cotyledon) three days after

infection covering the epidermal cells in these zones (Figure 7g-i). To observe the presence of mycelium underneath the epidermis, we transversally cut the roots and stems using a sharp single-edged razor blade and immediately observed the freshly cut surface using the ESEM. The external structures of the transversally-cut roots, including cortex and epidermis cells did not withstand the vacuum and collapsed, with the exception of the central cylinder retaining its structure (supplemental Figure S5). To overcome the deformation of the freshly-cut sections and observe the sub-epidermal tissues and the fungus hyphae, the infected seedlings were plunge-frozen in liquid nitrogen, and then fractured in the root and hypocotyl regions as previously described (Wakui et al., 1999). The fractured surfaces of roots and hypocotyls then were instantly observed in low vacuum mode at ≈1 torr to elucidate the presence of fungus in the internal structure of plantlets. Preparation of these tissues by freeze-fracturing could preserve their overall structure and components such as the epidermal and cortex cells and vascular cylinder, and allowed detection of fungal mycelium in the internal surfaces of roots (Figure 7j-l). These images showed that the hyphae could penetrate into the cortical cells, that could later colonize the vascular tissue of the plants as previously shown by bright-field and fluorescent images by Blum et al. (2018). Obviously, freeze-fracturing and low vacuum observation of the plant samples, did not preserve their vitality, but it was unavoidable to detect details of internal structure of tissues and to complement the ESEM observation of the external surfaces. These results, indeed, can be always supplemented by the conventional SEM analyses following classical sample preparations.

4. Conclusion

In this work, we modified a commercially available ESEM sample holder to observe and image live growing plantlets *in situ*. The use of newly designed and 3-D printed accessories in combination with optimized control of the relative humidity and tuning of imaging parameters permitted maintaining the plant seedlings viable during observation and acquiring quality ESEM images. This approach allowed us to observe structural modification of cells in living plantlets upon the application of a biopolymer-modifying enzyme or interaction with a fungus. These novel *in situ* ESEM observations are largely comparable to those made on cryo-prepared samples using low-vacuum SEM and light microscopy. Therefore, we conclude that our adopted approach in using ESEM for *in situ* analysis of the surfaces of living plantlets is a reliable means of assessing their evolution and growth, modification by enzymes, or

degradation by fungi at cellular levels. There is clearly considerable scope to use this method to examine the interaction of various physical, chemical and biological agencies with surfaces of living plants or other biological samples. However, maintaining the humidity and viability of samples during the ESEM observations, imposed some limitations such as smaller field of view and shorter observation timespan compared to conventional SEM. Further research will address the technical limitations of this approach by employing technologies currently commercially available, such as micromanipulators and in-chamber optical cameras for faster sample navigation or novel detection systems, and developing more sample-specific accessories to expand the application of *in situ* ESEM into the relevant fields.

Funding

This research was funded by the Région Hauts-de-France, through the ENSEMBLE project (120-2016 RDIPROJINV-000083 RDIPROJFT-000192).

Acknowledgements

The authors thank “Région Hauts-de-France” for its financial support. Arash Jamali and Romain Roulard are grateful to Dr. Sylvain Lecomte at the ““Linéa Semences” for his helpful advice in the application of fungi for artificial contamination of flax plantlets. Arash Jamali would like to thank Dr. Emmanuelle Etienne from “Direction de la Recherche ” at Université de Picardie Jules Verne for her administrative assistance and advice in this research project.

Reference

Babu, Y., Musielak, T., Henschen, A., Bayer, M., 2013. Suspensor length determines developmental progression of the embryo in *arabidopsis*. Plant Physiol. 162, 1448-1458. https://doi.org/10.1104/pp.113.217166

Barbier de Reuille, P., Bohn-Courseau, I., Godin, C., Traas, J., 2005. A protocol to analyse cellular dynamics during plant development. Plant J. 44, 1045-1053. https://doi.org/10.1111/j.1365-313X.2005.02576.x

Berhin, A., de Bellis, D., Franke, R.B., Buono, R.A., Nowack, M.K., Nawrath, C., 2019. The root cap cuticle: A cell wall structure for seedling establishment and lateral root formation. Cell 176, 1367-1378.e1368. https://doi.org/10.1016/j.cell.2019.01.005

Blum, A., Bressan, M., Zahid, A., Trinsoutrot-Gattin, I., Driouich, A., Laval, K., 2018. Verticillium wilt on fiber flax: Symptoms and pathogen development in planta. Plant Dis. 102, 2421-2429. https://doi.org/10.1094/PDIS-01-18-0139-RE

Bogner, A., Jouneau, P.H., Thollet, G., Basset, D., Gauthier, C., 2007. A history of scanning electron microscopy developments: Towards “wet-stem” imaging. Micron. 38, 390-401. https://doi.org/10.1016/j.micron.2006.06.008

Bozzola, J.J., Russell, L.D., 1999. Electron microscopy: Principles and techniques for biologists, second ed. Jones & Bartlett Learning, p. 670

Burgert, I., Keplinger, T., 2013. Plant micro- and nanomechanics: Experimental techniques for plant cell-wall analysis. J. Exp. Bot. 64, 4635-4649. https://doi.org/10.1093/jxb/ert255

Byrne, M.E., 2006. Shoot meristem function and leaf polarity: The role of class iii hd-zip genes. PLoS Genet. 2, e89. https://doi.org/10.1371/journal.pgen.0020089

Carr, S.G.M., Carr, D.J., 1975. Intercellular pectic strands in parenchyma: Studies of plant cell walls by scanning electron microscopy. Aust. J. Bot. 23, 95-105. https://doi.org/10.1071/BT9750095

Costa, G., Plazanet, I., 2016. Plant cell wall, a challenge for its characterisation. A.B.C. 6, 70-105. https://doi.org/10.4236/abc.2016.63008

Dauwe, R., Roulard, R., Ramos, M., Thiombiano, B., Mesnard, F., Gontier, E., Jamali, A., 2021. Etching of the seed cuticle by cold plasma shortens imbibitional leakage in *linum usitatissimum* L. Ind. Crops. Prod. 167, 113536. https://doi.org/10.1016/j.indcrop.2021.113536

Desnos, T., Orbovic, V., Bellini, C., Kronenberger, J., Caboche, M., Traas, J., Hofte, H., 1996. *Procuste1* mutants identify two distinct genetic pathways controlling hypocotyl cell elongation, respectively in dark- and light-grown *arabidopsis* seedlings. Development. 122, 683-693. https://doi.org/10.1242/dev.122.2.683

Dobberstein, H., Purser, N., Fairhead, T., Stokes, D., Knowles, R., 2005. Beam blanking studies in environmental scanning electron microscopy. Microsc. Microanal. 11, 400-401. https://doi.org/10.1017/S1431927605507748

Donald, A., Baker, F., Smith, A., Waldron, K., 2003. Fracture of plant tissues and walls as visualized by environmental scanning electron microscopy. Ann. Bot. 92, 73-77. https://doi.org/10.1093/aob/mcg115

Donald, A.M., 2003. The use of environmental scanning electron microscopy for imaging wet and insulating materials. Nat. Mater. 2, 511-516. 10.1038/nmat898

523 Ensikat, H., Ditsche-Kuru, P., Barthlott, W., Méndez-Vilas, A., 2010. Scanning electron
524 microscopy of plant surfaces: Simple but sophisticated methods for preparation and
525 examination, in: Méndez-Vilas, A., Diaz, J. (Eds.), Microscopy: Science, technology,
526 applications and education. Formatex, pp. 248-255.

527 FEI Company, 2010. The quanta feg user operation manual. , FEI company, USA.

528 Gendreau, E., Traas, J., Desnos, T., Grandjean, O., Caboche, M., Hofte, H., 1997. Cellular basis
529 of hypocotyl growth in arabidopsis thaliana. Plant Physiol. 114, 295-305.
530 https://doi.org/10.1104/pp.114.1.295

531 Gilpin, C.J., 1997. Biological applications of environmental scanning electron microscopy.
532 Microsc. Microanal. 3, 383-384. https://doi.org/10.1017/S1431927600008801

533 He, Y., Zhou, K., Wu, Z., Li, B., Fu, J., Lin, C., Jiang, D., 2019. Highly efficient nanoscale analysis
534 of plant stomata and cell surface using polyaddition silicone rubber. Front. Plant Sci. 10.
535 https://doi.org/10.3389/fpls.2019.01569

536 Holland, C., Ryden, P., Edwards, C.H., Grundy, M.M.-L., 2020. Plant cell walls: Impact on
537 nutrient bioaccessibility and digestibility. Foods. 9, 201.
538 https://doi.org/10.3390/foods9020201

539 Inderbitzin, P., Bostock, R.M., Davis, R.M., Usami, T., Platt, H.W., Subbarao, K.V., 2011.
540 Phylogenetics and taxonomy of the fungal vascular wilt pathogen *verticillium*, with the
541 descriptions of five new species. PloS one. 6, e28341.
542 https://doi.org/10.1371/journal.pone.0028341

543 Jacq, A., Pernot, C., Martinez, Y., Domergue, F., Payré, B., Jamet, E., Burlat, V., Pacquit, V.B.,
544 2017. The arabidopsis lipid transfer protein 2 (atltp2) is involved in cuticle-cell wall interface
545 integrity and in etiolated hypocotyl permeability. Front Plant Sci 8, 263-263.
546 https://doi.org/10.3389/fpls.2017.00263

547 Jansson, A., Nafari, A., Sanz-Velasco, A., Svensson, K., Gustafsson, S., Hermansson, A.-M.,
548 Olsson, E., 2013. Novel method for controlled wetting of materials in the environmental
549 scanning electron microscope. Microsc. Microanal. 19, 30-37.
550 https://doi.org/10.1017/S1431927612013815

551 Jenkins, L.M., Donald, A.M., 2000. Observing fibers swelling in water with an environmental
552 scanning electron microscope. Text. Res. J. 70, 269-276.
553 https://doi.org/10.1177/004051750007000315

554 Jhala, A.J., Hall, L.M., 2010. Flax (*linum usitatissimum* L.): Current uses and future applications.
555 Aust. J. basic Appl. Sci. 4, 4304-4312.

556 Kaminskyj, S.G., Dahms, T.E., 2008. High spatial resolution surface imaging and analysis of
557 fungal cells using SEM and AFM. Micron. 39, 349-361.
558 https://doi.org/10.1016/j.micron.2007.10.023

559 Kirk, S., Skepper, J., Donald, A., 2009. Application of environmental scanning electron
560 microscopy to determine biological surface structure. J. Microsc. 233, 205-224.
561 https://doi.org/10.1111/j.1365-2818.2009.03111.x

562 Kumar, M., Campbell, L., Turner, S., 2016. Secondary cell walls: Biosynthesis and manipulation.
563 J. Exp. Bot. 67, 515-531. https://doi.org/10.1093/jxb/erv533

564 Kwon, Y.-E., Kim, J.-K., Kim, Y.-j., Kim, J.-G., Kim, Y.-J., 2019. Development of SEM and stem-in-
565 SEM grid holders for eds analysis and their applications to apatite phases. J. Anal. Sci. Technol.
566 10, 1-8. https://doi.org/10.1186/s40543-019-0186-0

567 Mayo, S.C., Chen, F., Evans, R., 2010. Micron-scale 3d imaging of wood and plant
568 microstructure using high-resolution x-ray phase-contrast microtomography. J. Struct. Biol.
569 171, 182-188. https://doi.org/10.1016/j.jsb.2010.04.001

570 McGregor, J., Donald, A., 2010. ESEM imaging of dynamic biological processes: The closure of
571 stomatal pores. J. Microsc. 239, 135-141. https://doi.org/10.1111/j.1365-2818.2009.03351.x

572 Muscariello, L., Rosso, F., Marino, G., Giordano, A., Barbarisi, M., Cafiero, G., Barbarisi, A.,
573 2005. A critical overview of ESEM applications in the biological field. J. Cell. Physiol. 205, 328-
574 334. https://doi.org/10.1002/jcp.20444

575 Oliver, M.J., 1996. Desiccation tolerance in vegetative plant cells. Physiol. Plant. 97, 779-787.
576 https://doi.org/10.1111/j.1399-3054.1996.tb00544.x

577 Pathan, A.K., Bond, J., Gaskin, R.E., 2010. Sample preparation for SEM of plant surfaces. Mater.
578 Today. 12, 32-43. https://doi.org/10.1016/S1369-7021(10)70143-7

579 Pillitteri, L.J., Dong, J., 2013. Stomatal development in *arabidopsis*. Arabidopsis Book. 11,
580 e0162-e0162. https://doi.org/10.1199/tab.0162

581 Popielarska-Konieczna, M., Bohdanowicz, J., Starnawska, E., 2010. Extracellular matrix of plant
582 callus tissue visualized by ESEM and SEM. Protoplasma. 247, 121-125.
583 https://doi.org/10.1007/s00709-010-0149-1

584 Sénéchal, F., Wattier, C., Rustérucci, C., Pelloux, J., 2014. Homogalacturonan-modifying
585 enzymes: Structure, expression, and roles in plants. J. Exp. Bot. 65, 5125-5160.
586 https://doi.org/10.1093/jxb/eru272

Shourideh, A.H., Bou Ajram, W., Al Lami, J., Haggag, S., Mansouri, A., 2018. A comprehensive study of an atmospheric water generator using peltier effect. Therm. Sci. Eng. Prog. 6, 14-26. https://doi.org/10.1016/j.tsep.2018.02.015

Sorbo, S., Basile, A., Castaldo Cobianchi, R., 2008. Applications of environmental scanning electron microscopy (ESEM) in botanical research. Plant Biosyst. 142, 355-359. https://doi.org/10.1080/11263500802150829

Sozzani, R., Busch, W., Spalding, E.P., Benfey, P.N., 2014. Advanced imaging techniques for the study of plant growth and development. Trends Plant Sci. 19, 304-310. https://doi.org/10.1016/j.tplants.2013.12.003

Stabentheiner, E., Zankel, A., Pölt, P., 2010. Environmental scanning electron microscopy (ESEM)—a versatile tool in studying plants. Protoplasma. 246, 89-99. https://doi.org/10.1007/s00709-010-0155-3

Stant, M.Y., 1973. The role of the scanning electron microscope in plant anatomy. Kew Bull. 28, 105-115. https://doi.org/10.2307/4117068

Stokes, D., 2008. Principles and practice of variable pressure/environmental scanning electron microscopy (vp-ESEM). John Wiley & Sons, UK, UK, p. 234.

Talbot, M.J., White, R.G., 2013. Cell surface and cell outline imaging in plant tissues using the backscattered electron detector in a variable pressure scanning electron microscope. Plant Methods. 9, 40. https://doi.org/10.1186/1746-4811-9-40

The *Arabidopsis* Genome Initiative, 2000. Analysis of the genome sequence of the flowering plant *arabidopsis thaliana*. Nature. 408, 796-815. https://doi.org/10.1038/35048692

Tihlaříková, E., Neděla, V., Đorđević, B., 2019. In-situ preparation of plant samples in ESEM for energy dispersive x-ray microanalysis and repetitive observation in SEM and ESEM. Sci. Rep. 9, 1-8. https://doi.org/10.1038/s41598-019-38835-w

Toole, E.H., Toole, V.K., Borthwick, H.A., Hendricks, S.B., 1955. Interaction of temperature and light in germination of seeds. Plant Physiol. 30, 473-478. https://doi.org/10.1104/pp.30.5.473

Treitel, O., 1949. Elasticity, plasticity, water content, and hardness of plant tissues of different ages. Trans. Kans. Acad. Sci. 52, 219-231. https://doi.org/10.2307/3626173

Tsukaya, H., 2013. Leaf development. Arabidopsis Book. 11, e0163-e0163. https://doi.org/10.1199/tab.0163

618 Vicré, M., Farrant, J.M., Driouich, A., 2004. Insights into the cellular mechanisms of desiccation
619 tolerance among angiosperm resurrection plant species. Plant Cell Environ. 27, 1329-1340.
620 https://doi.org/10.1111/j.1365-3040.2004.01212.x

621 Vogler, H., Felekis, D., Nelson, B.J., Grossniklaus, U., 2015. Measuring the mechanical
622 properties of plant cell walls. Plants. 4, 167-182. https://doi.org/10.3390/plants4020167

623 Wakui, K., Takahata, Y., Kaizuma, N., 1999. Scanning electron microscopy of desiccation-
624 tolerant and-sensitive microspore-derived embryos of *brassica napus* L. Plant Cell Rep. 18,
625 595-600. https://doi.org/10.1007/s002990050628

626 Wang, H., Qiu, C., Abbasi, A.M., Chen, G., You, L., Li, T., Fu, X., Wang, Y., Guo, X., Liu, R.H., 2015.
627 Effect of germination on vitamin c, phenolic compounds and antioxidant activity in flaxseed
628 (*linum usitatissimum* L.). Int. J. Food Sci. Technol. 50, 2545-2553.
629 https://doi.org/10.1111/ijfs.12922

630 Wang, H., Wang, J., Guo, X., Brennan, C.S., Li, T., Fu, X., Chen, G., Liu, R.H., 2016. Effect of
631 germination on lignan biosynthesis, and antioxidant and antiproliferative activities in flaxseed
632 (*linum usitatissimum* L.). Food Chem. 205, 170-177.
633 https://doi.org/10.1016/j.foodchem.2016.03.001

634 Wigzell, J.M., Racovita, R.C., Stentiford, B.G., Wilson, M., Harris, M.T., Fletcher, I.W., Mosquin,
635 D.P.K., Justice, D., Beaumont, S.K., Jetter, R., Badyal, J.P.S., 2016. Smart water channelling
636 through dual wettability by leaves of the bamboo *phyllostachys aurea*. Colloids Surf. A
637 Physicochem. Eng. Asp. 506, 344-355. https://doi.org/10.1016/j.colsurfa.2016.06.058

638 Wu, B., Becker, J.S., 2012. Imaging techniques for elements and element species in plant
639 science. Metallomics. 4, 403-416. https://doi.org/10.1039/c2mt00002d

640 Yeats, T.H., Rose, J.K.C., 2013. The formation and function of plant cuticles. Plant Physiol 163,
641 5-20. https://doi.org/10.1104/pp.113.222737

642 Zhang, G., Hou, X., Wang, L., Xu, J., Chen, J., Fu, X., Shen, N., Nian, J., Jiang, Z., Hu, J., Zhu, L.,
643 Rao, Y., Shi, Y., Ren, D., Dong, G., Gao, Z., Guo, L., Qian, Q., Luan, S., 2021. Photo-sensitive leaf
644 rolling 1 encodes a polygalacturonase that modifies cell wall structure and drought tolerance
645 in rice. New Phytol. 229, 890-901. https://doi.org/10.1111/nph.16899

646 Zhang, Z., Zhou, Y., Zhu, X., Fei, L., Huang, H., Wang, Y., 2020. Applications of ESEM on
647 materials science: Recent updates and a look forward. Small Methods. 4, 1900588.
648 https://doi.org/10.1002/smtd.201900588

649 Zheng, T., Waldron, K., Donald, A.M., 2009. Investigation of viability of plant tissue in the
650 environmental scanning electron microscopy. Planta. 230, 1105-1113.
651 https://doi.org/10.1007/s00425-009-1009-0

652

653 **Figure and Table captions**

654 **Figure 1**: Standard cooling stage module: (a) cooling stage (Peltier/Seebeck) assembly
655 containing a standard ESEM sample holder, installed on the stage of the Quanta 200 ESEM
656 chamber, (b) the image and dimensions of a standard ESEM sample holder, and (c) a 3-days
657 old *Arabidopsis* plantlet (arrowed in upper image) and a flaxseed (arrowed in lower image)
658 showing their size relative to the standard holder's surfaces. The yellow arrows in b and c
659 indicate the width of the edge of the holder

660

661 **Figure 2**: Comparison of the standard cooling stage with the new-designed module and their
662 sample holders. Modification of the standard cooling stage (Peltier/Seebeck) (a) increased the
663 mount-receiving surface (emplacement of sample holder) from 1 cm^2 to 5 cm^2 (b). Technical
664 details on this modification are provided in Supplemental Figures of this article

665

666 **Figure 3**: The effect of chamber pump-down and relative humidity on the structure of a very
667 young (2-days old) hydrated *Arabisopsis* seedling: (a) a low magnification image of an entire
668 seedling taken at a long working distance showing the dehydrated cells, (b-d) higher
669 magnification images of different organs of the same plant, showing the deformation of the
670 cell walls in testa, root and hypocotyl, (e-g) images of the hypocotyls showing the effect of
671 chamber's relative humidity in conservation of their structure during the ESEM observation;
672 note the structural deformation at RH lower than 75% (f) and water film formation and
673 submersion of the tissue at 100 % RH (g) (images were acquired at 5Torr and between 4 to
674 6°C)

675

676 **Figure 4**: ESEM observation of tissues and cells of seeds and young seedlings of *Arabidopsis*
677 following optimization of the chamber and imaging parameters: (a) observation of a seed, (b)
678 cullumola of the mucileagous cells, (c) endothelial cells at the micropylar region in a 2-day
679 germinating seed, (d) overall view of an entire plantlet (e) cotyledon (leaves within the embryo
680 of the seed), (f) apical hook, (g) higher magnification image of a cotyledon showing a jigsaw
681 puzzle arrangement stomatal and non stomatal cells, (h) meristematic and transition zones of

682 the primary root apical meristem, (i) rhizoderm cells and extremely delicate root hairs (tubular
683 elongations of the root epidermis (rhizodermis)), (j & k) the shoot apical meristem positioned
684 between the two cotyledons, (l) marginal elongated epidermal cells seen parallel to the
685 cotyledon edges, (m, n and o) vegetative apex showing the adaxial side of the leaf adjacent to
686 the central shoot apical meristem and the presence of trichomes indicating dorsoventrality

687

688 **Figure 5**: ESEM observation of flax plantlets during their early stage of growth starting from
689 second day after the seed germination in the "bio-chamber". Each row includes a photograph
690 and examples of ESEM micrographs acquired from different parts of the growing plantlets at
691 a specific day (D) after germination; D2: hypocotyl (a) and remaining of a single cell
692 endosperm layer (b and c); D5: cotyledon (a), hypocotyl (b) and individual angular cells of
693 endosperm layer (c); D7: epidermal cells at apical hook zone of a hypocotyl showing the lines
694 containing protruding cells (a), abaxial epidermis of cotyledon with the pavement cells and
695 stomata (b), and a higher magnification image of a stomata showing its guard cells (c); D9:
696 epidermal cells and stomata on hypocotyl (a), zone of the hypocotyl showing the view of an
697 epidermal meristem (b), epidermal cells of cotyledons (c); D12: parallel lines of protruding
698 epidermal cells on the hypocotyl (a), the shoot apical meristem (b), and abaxial epidermis with
699 the pavement cells and stomata (c)

700

701 **Figure 6**: Structural modification of 4 day-old dark-grown *Arabidopsis* hypocotyls resulting
702 from the application of AtPGLR enzyme. ESEM images (first row) of hypocotyls treated with
703 either inactivated enzyme showing no structural modification (a) or an active enzyme showing
704 deformation and longitudinal separation of the walls of epidermal and underlying cortex cells
705 (b and c). Second and third rows are images acquired by low vacuum SEM of cryo-prepared
706 samples and light microscopy, respectively, showing hypocotyls treated either with
707 inactivated (d and g) or active enzymes (e, f, h and i); note their high comparability with ESEM
708 images

709

710 **Figure 7**: Fungus *Verticilium dahliae* in the culture medium and colonization of the artificially
711 infected flax plantlets; *In situ* ESEM observation of vegetative mycelium of *V. dhaliae* in the

712 culture medium showing the mycelium network (microsclerotia) (a) and different hyphal
713 structures such as conidia, conidiophores and phialides in the fungal colony (b and c);
714 observation of the roots in artificially infected plants in day one after infection showing a thick
715 mantle of closely interlaced hyphae covering the Rhizodermis cells (d, e and f); hypocotyl of
716 an infected flax plantlet showing the fungal hyphae covering the epidermis cells (g), stomata
717 (arrowed in h) and remaining of endosperm layer 3days after infection (i); freeze-fracturing of
718 a 21 days-old flax plantlet root, 3days after their artificial infection by *V. dahliae* (j-l), low
719 vacuum SEM revealing the presence of fungi mycelium on the external surfaces (j and k) and
720 its penetration into the sub-epidermal cells (arrowed in l)

721

722 **Table 1**: Summary of the optimal parameters for Low vacuum (LoVac) and Environmental SEM
723 (ESEM) observations of tissues of living plantlets and fungus

724

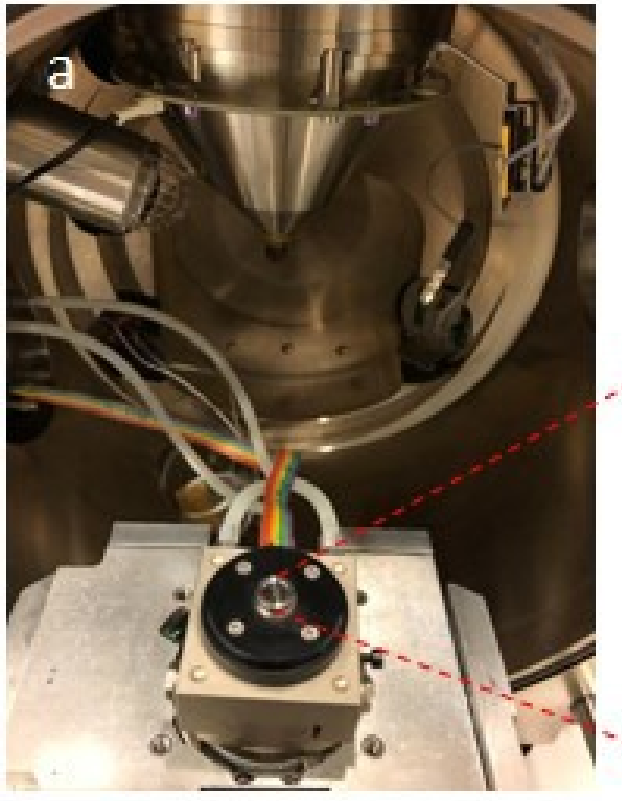
a

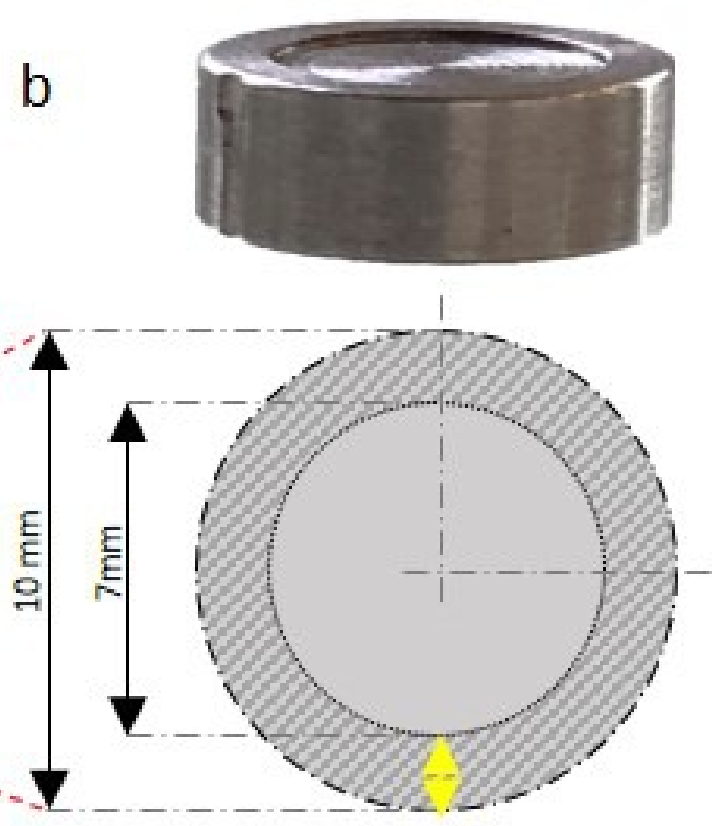
b
10 mm
7mm

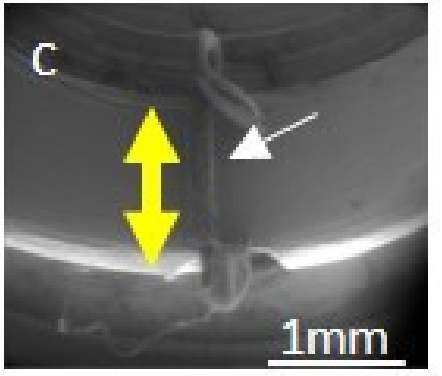
c
1mm

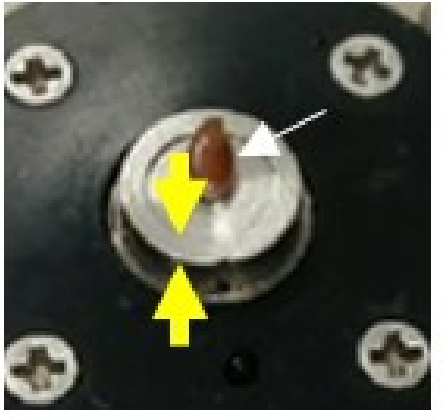

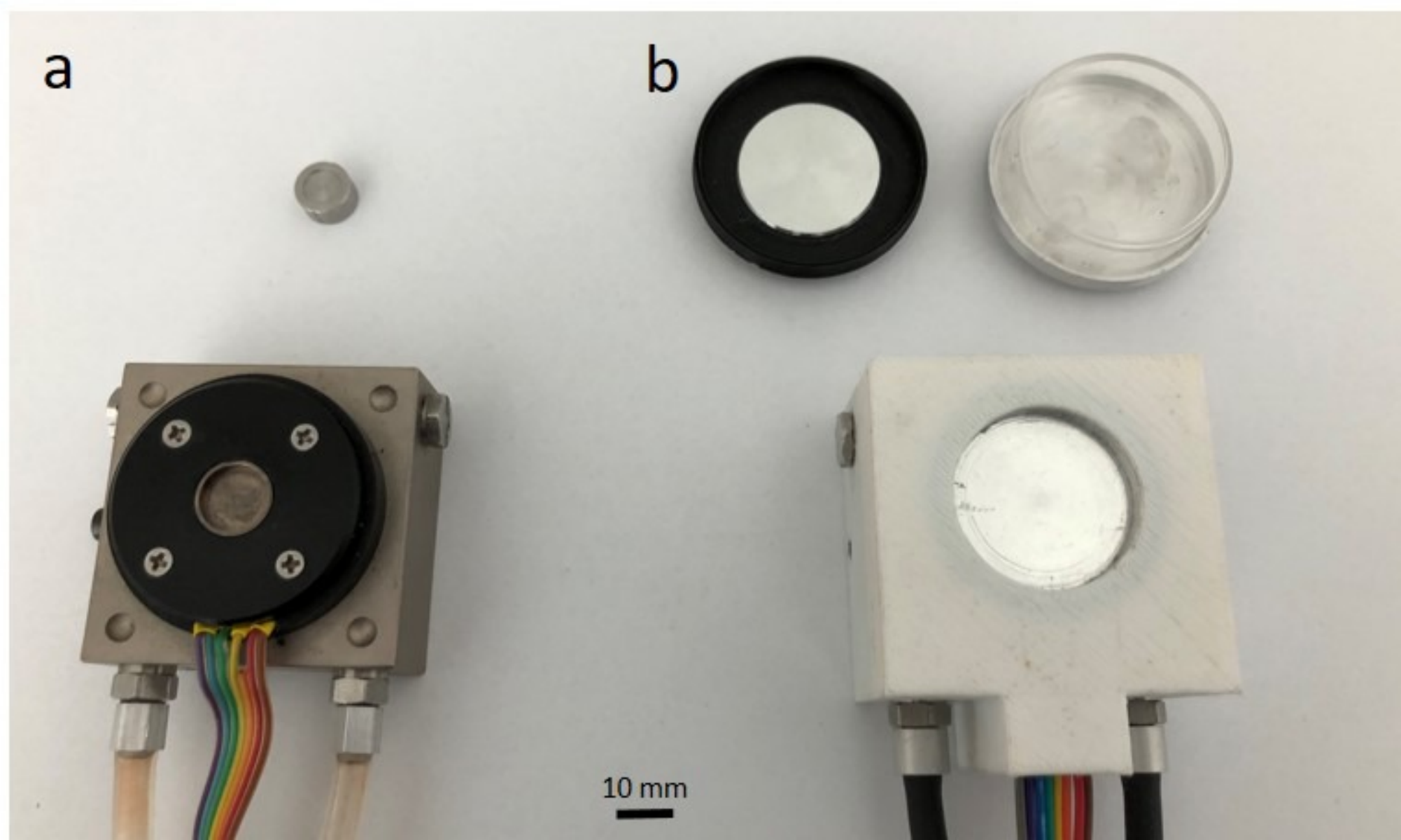
a
b
10 mm

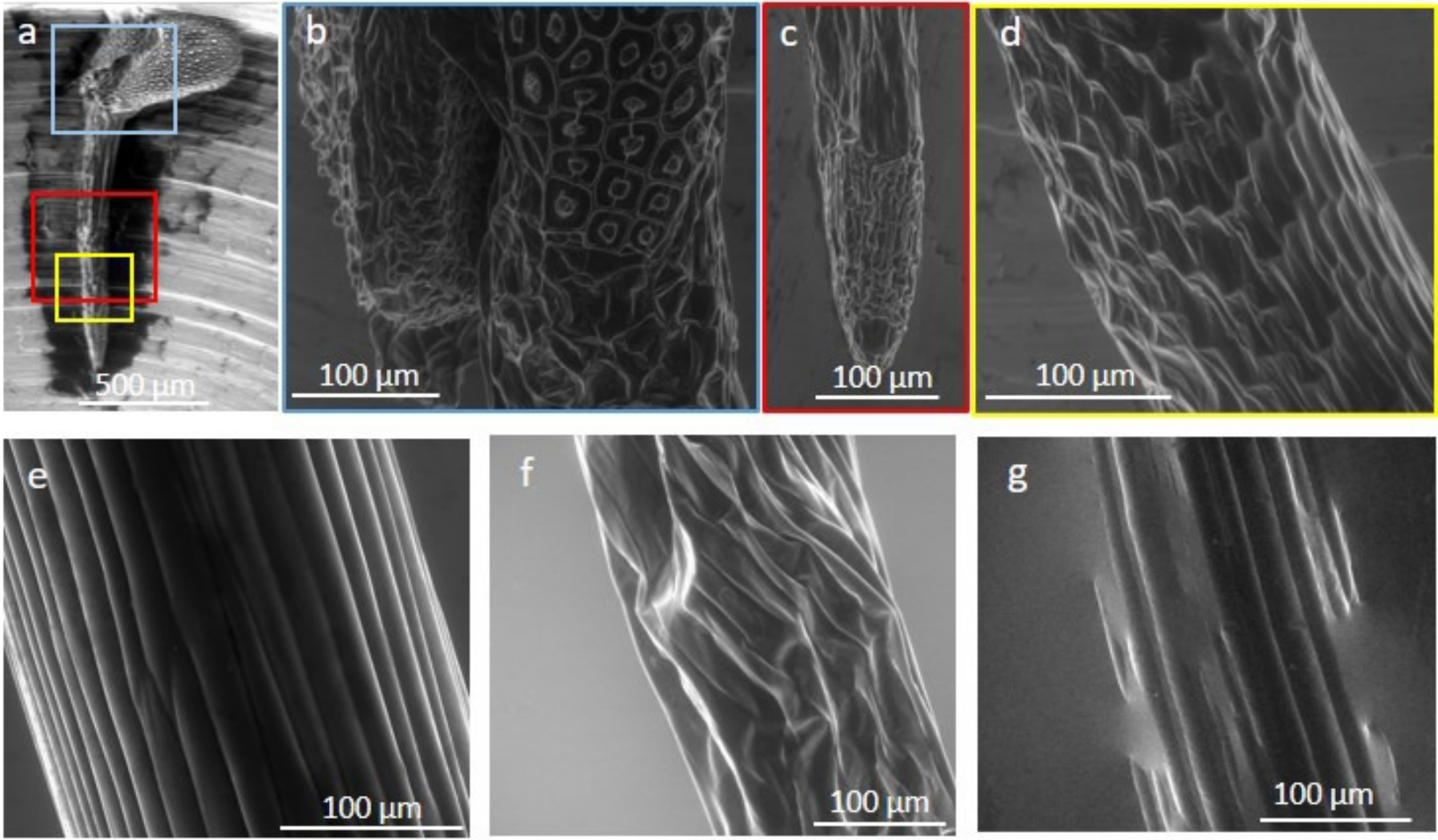
a
500 µm
b
100 µm
c
100 µm
d
100 µm
e
100 µm
f
100 µm
g
100 µm

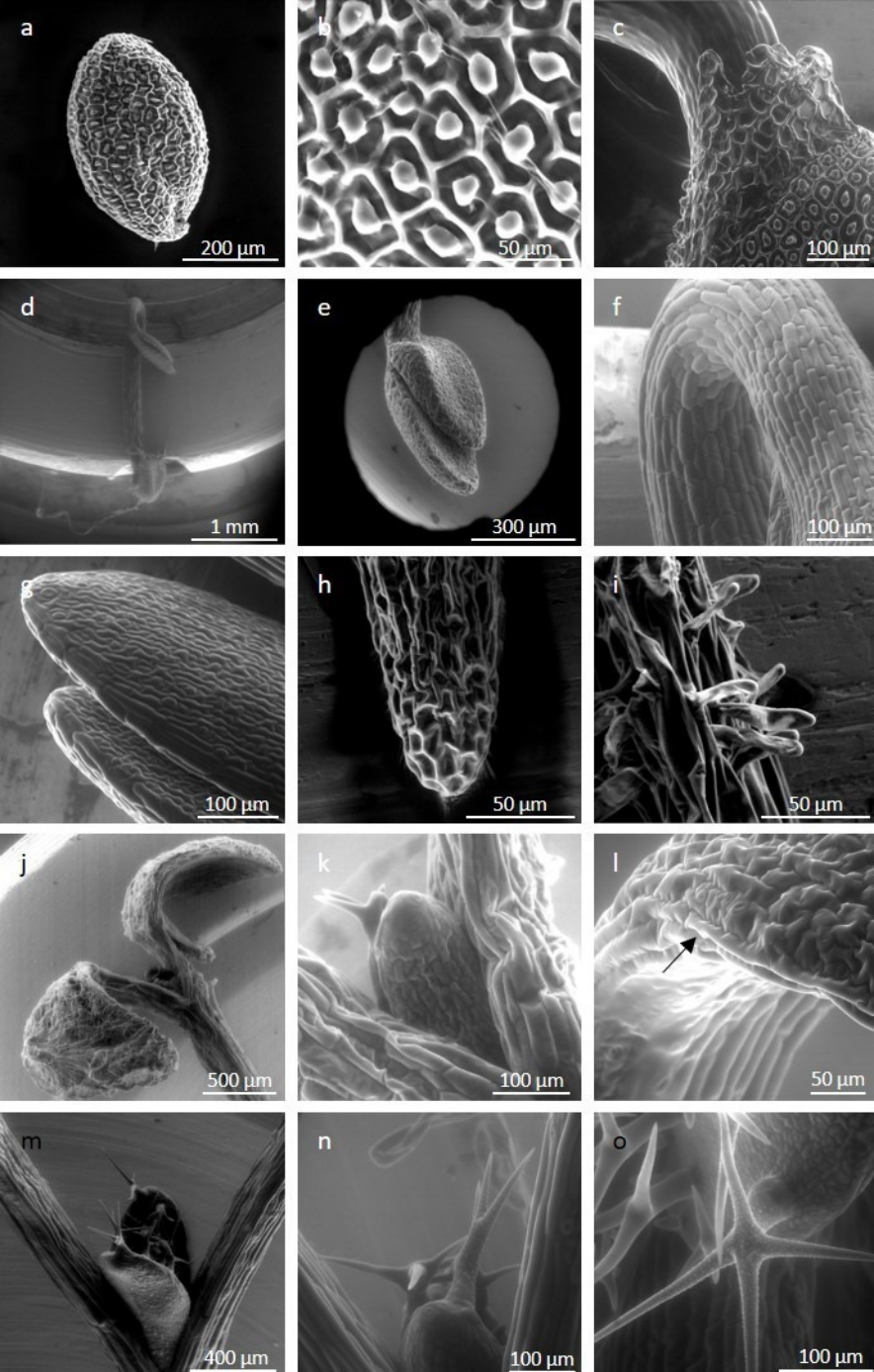
a
200 µm
b
50 µm
c
100 µm
d
1 mm
e
300 µm
f
100 µm
g
100 µm
h
50 µm
i
50 µm
j
500 µm
k
100 µm
l
50 µm
m
400 µm
n
100 µm
o
100 µm

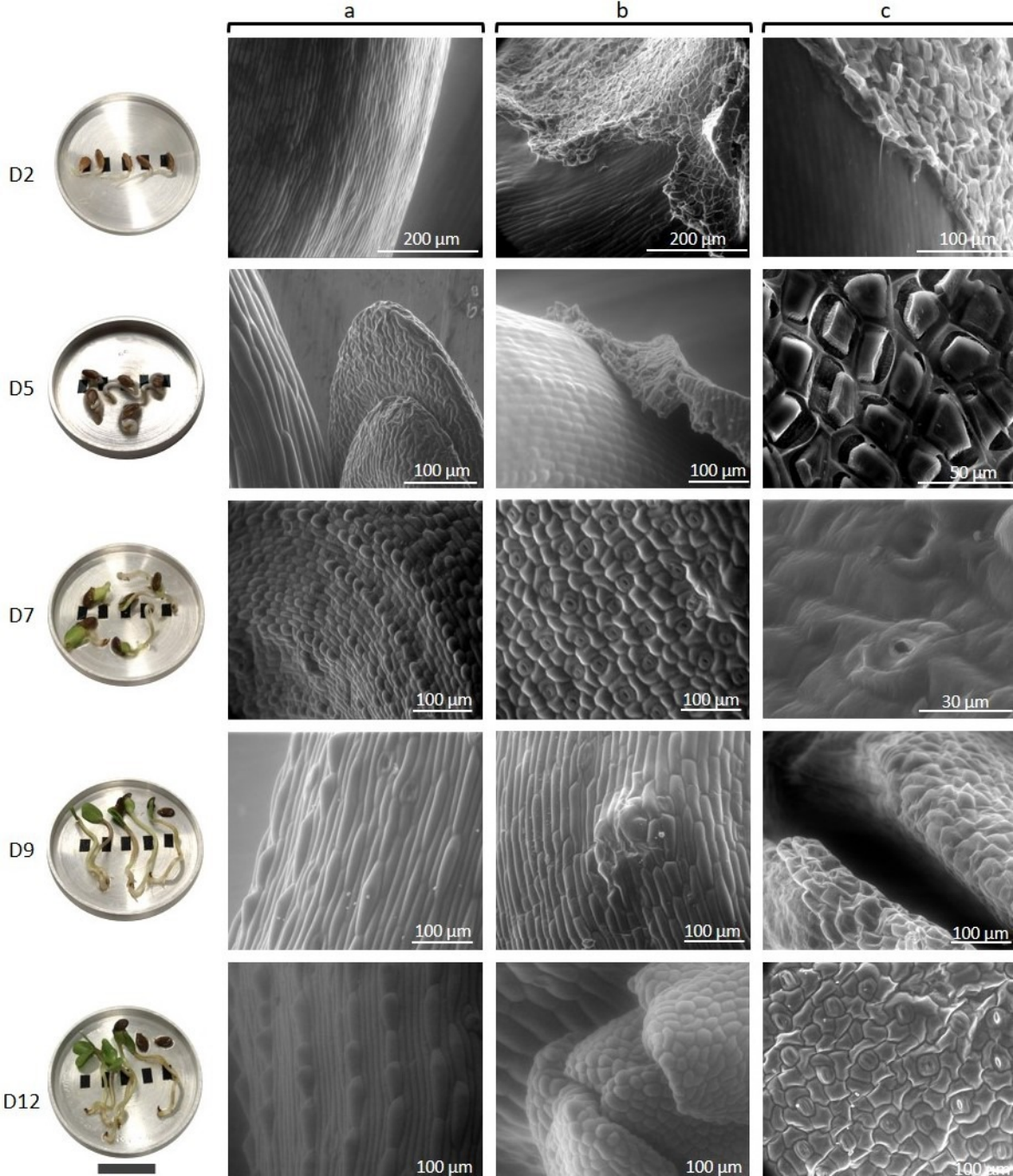
a
b
c
D2
D5
D7
D9
D12
200 µm
200 µm
100 µm
100 µm
100 µm
50 µm
100 µm
100 µm
30 µm
100 µm
100 µm
100 µm
100 µm
100 µm
100 µm

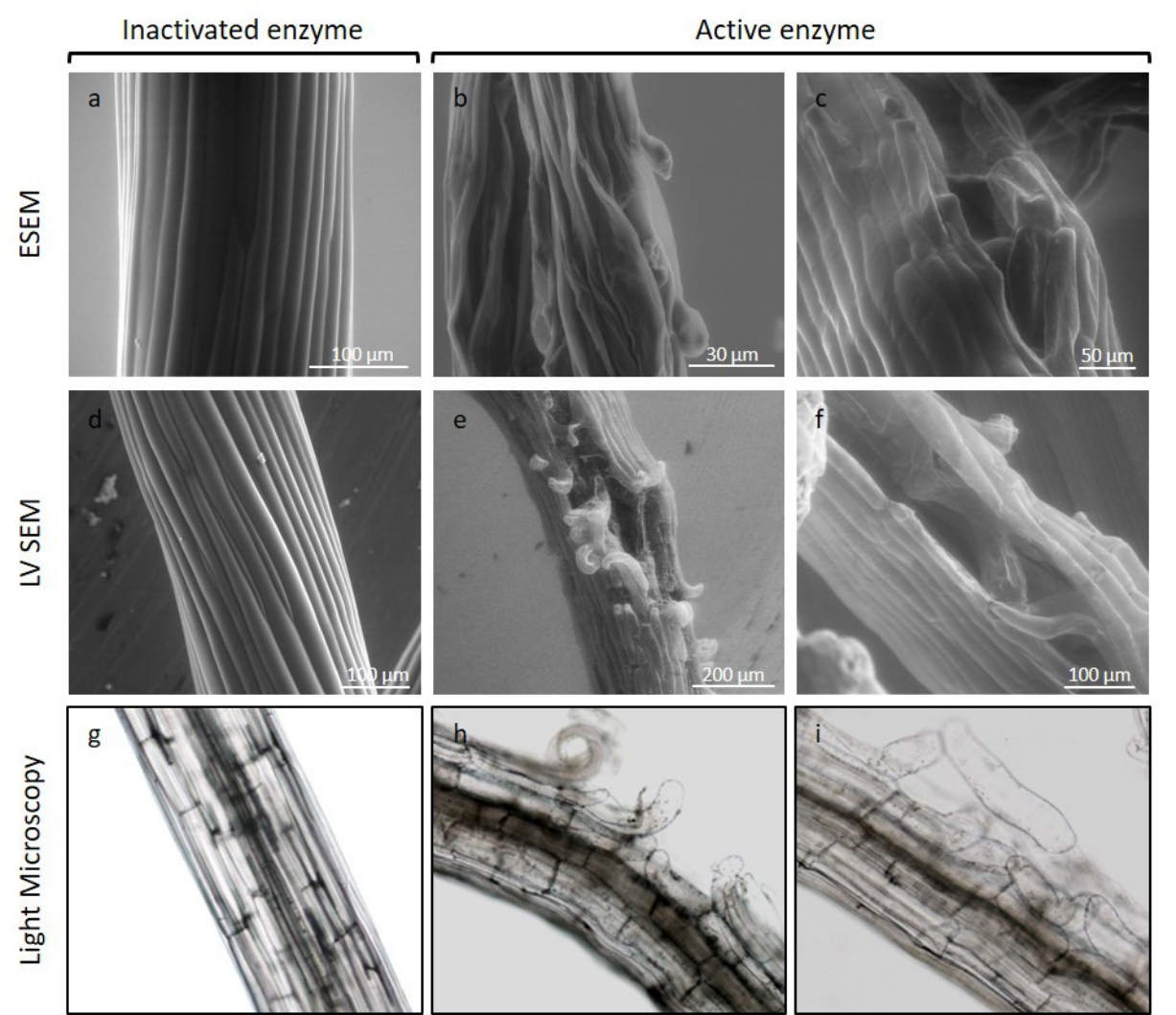
Inactivated enzyme
Active enzyme
ESEM
LV SEM
Light Microscopy
a
b
c
d
e
f
g
h
i
100 µm
30 µm
50 µm
100 µm
200 µm
100 µm

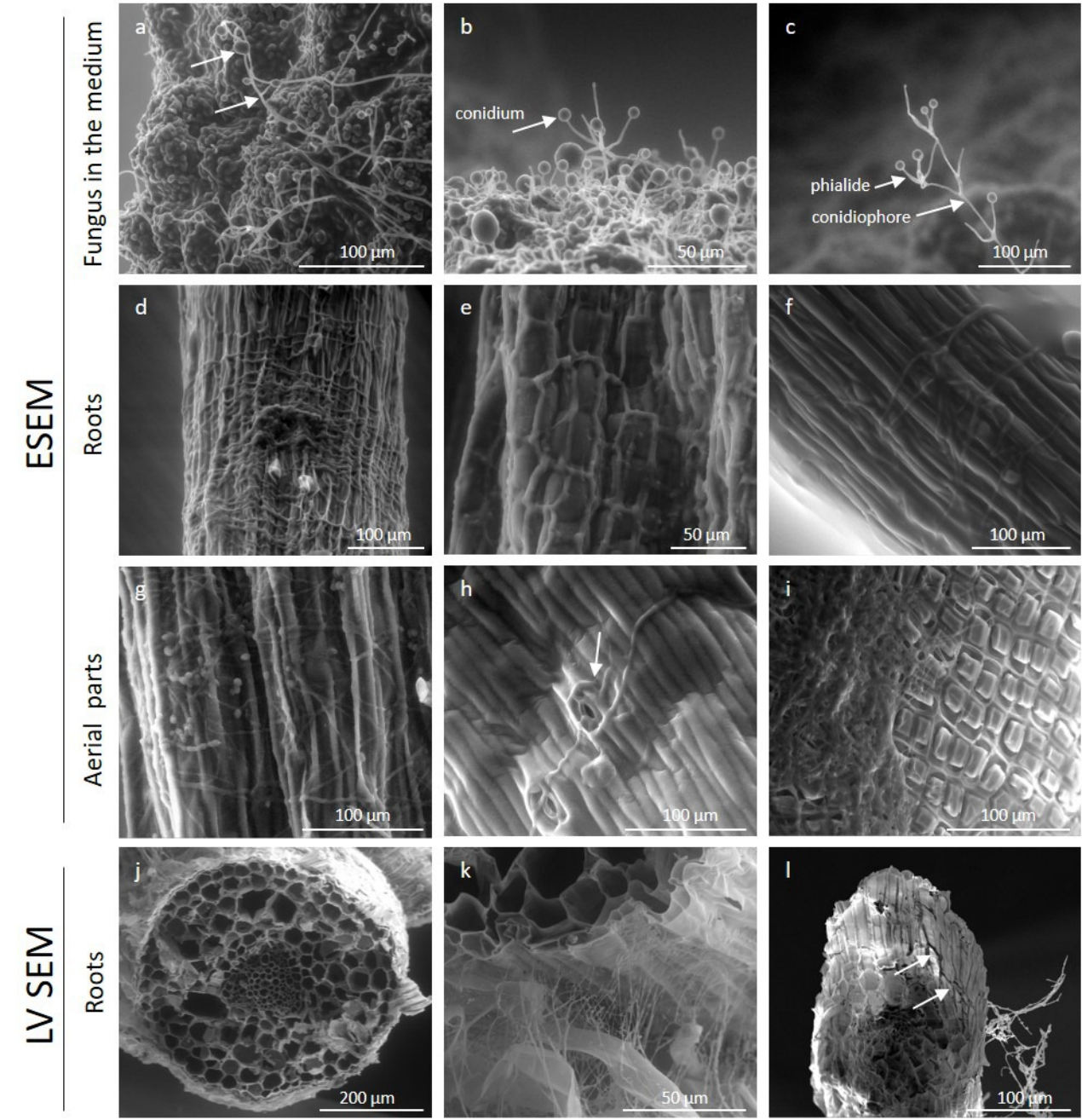
ESEM
LV SEM
Fungus in the medium
Roots
Aerial parts
Roots
a
b
c
d
e
f
g
h
i
j
k
l
conidium
phialide
conidiophore
100 µm
50 µm
200 µm

Samples		Operational mode	Accelerating voltage, kV	Magnification	Working Distance, mm	Vapor pressure, Torr (Pa)	Spot size	Temprature, C°/relative Humidity %
Arabidopsis†	Seeds	LoVac	5	500-1000	5	0,75 (100)	3	-
	Hypocotyls	ESEM	5-10	350 - 4000	4-5 mm	13-15 (1733-2000)	3.5	18-20/85-100
	Leaves	ESEM	15-20	500	5,5	14 (1867)	4,5	20/80
	Trichomes	ESEM	5	500	6	15 (2000)	3,5	20/75
Fungus††		ESEM	15	500-800	5,5	12 (1600)	4	19/70-75
Flax†††	Roots	ESEM	10-15	500-1000	6,5	6,5 (867)	3,5	8/80
	Infected plantlets	ESEM	20	200-500	7,5	9 (1200)	4	18/60
	Freeze-fractured Tissues	LoVac	10	400-800	6-8	1 (133)	3	-

†*Arabidopsis thaliana (2 to 5-days old);* ††*Verticillium dahlia (grown for 5 to 7 days);* †††*Linum usitatissimum (2 to 5-days old)*


ESEM